

Comparison between relativistic, semirelativistic, and nonrelativistic approaches of quarkonium

C. Semay

Université de Mons-Hainaut, Faculté des Sciences, 19 Avenue Maistriau, B-7000 Mons, Belgium

B. Silvestre-Brac

Institut des Sciences Nucléaires, 53 Avenue des Martyrs, F-38026 Grenoble Cédex, France

(Received 11 May 1992)

We study the connections existing between relativistic, semirelativistic, and nonrelativistic potential models of quarkonium using an interaction composed of an attractive Coulomb potential and a confining power-law term. We show that the spectra of these very different models become nearly similar provided specific relations exist between the dimensionless parameters peculiar to each model. As our analysis is carried out by taking advantage of scaling laws, our results are applicable for a wide range of physical parameters.

PACS number(s): 12.40.Qq, 03.65.Ge, 11.10.Qr, 14.40.-n

I. INTRODUCTION

Some recent works [1,2] shed some light on the theoretical interpretation of the potential models of QCD. These models are convenient tools to calculate most properties of hadrons. Acceptable results are provided by relativistic as well as by nonrelativistic approaches [3-5]. Both types of models use generally the same kind of "QCD-inspired" interaction, namely, a short-range part dominated by one-gluon exchange and a confining long-range part described by a power-law potential. However, they differ drastically in quark mass and kinematics: while in the nonrelativistic models the light quarks (u, d) have mass of the order of one-third of the nucleon mass and obey a Schrödinger equation, in the other models the light quarks have very small mass, and accordingly, their motion is ultrarelativistic.

Several works have been devoted to the comparison of nonrelativistic and relativistic quark models. Lucha and Schöberl [6] showed that the semirelativistic two-body Hamiltonian (in natural units $\hbar=c=1$)

$$H = \sqrt{\mathbf{p}^2 + m_1^2} + \sqrt{\mathbf{p}^2 + m_2^2} + V(\mathbf{r}) \quad (1.1)$$

can be approximately recast in the form of a nonrelativistic Hamiltonian

$$H_{nr} = \hat{m}_1 + \hat{m}_2 + \frac{\mathbf{p}^2}{2\hat{m}_1} + \frac{\mathbf{p}^2}{2\hat{m}_2} + V_{nr}(\mathbf{r}), \quad (1.2)$$

with effective masses $\hat{m}_i = \frac{1}{2}\sqrt{\langle \mathbf{p}^2 \rangle + m_i^2}$ and an effective potential

$$V_{nr} = V + \hat{m}_1 + \hat{m}_2 - \frac{\langle \mathbf{p}^2 \rangle}{2\hat{m}_1} - \frac{\langle \mathbf{p}^2 \rangle}{2\hat{m}_2}. \quad (1.3)$$

Consequently, the effective masses \hat{m}_i , and the effective potential V_{nr} , which depend on the average momentum $\langle \mathbf{p}^2 \rangle$, vary from level to level. But the authors point out that, in the nonrelativistic formalism, the virial theorem implies that $\langle \mathbf{p}^2 \rangle$ is a constant when the interaction is

reduced to a confining logarithmic potential. In this case the effective quantities \hat{m}_i and V_{nr} are independent of the level of excitation.

It was noted by Rosenstein [7] that the Schrödinger equation with linear potential

$$\left[\frac{\mathbf{p}^2}{2M} + br + a \right] \psi_n = E_n \psi_n \quad (1.4)$$

and the ultrarelativistic Klein-Gordon equation with a quadratic potential

$$(\sqrt{\mathbf{p}^2} + \frac{1}{2}\omega^3 r^2 + c) \phi_n = \epsilon_n \phi_n \quad (1.5)$$

transform to each other under the transformation $\mathbf{p} \rightarrow b\mathbf{r}$ and $\mathbf{r} \rightarrow \mathbf{p}/b$ provided $M\omega^3 = b^2$ and $a = c$. Therefore, the eigenvalues of these equations are the same and the wave functions are connected by the Fourier transform

$$\phi(\mathbf{r}) = \frac{1}{(2\pi)^{3/2}} \int e^{-i\mathbf{b}\mathbf{r}\cdot\mathbf{r}'} \psi(\mathbf{r}') d^3r'. \quad (1.6)$$

In the work of Ono [8], it is shown that a two-body Klein-Gordon equation, including a scalar potential $V_S(r)$ and a fourth component $V_V(r)$ of a four-vector potential, is formally identical to a Schrödinger equation supplemented by the effective energy-dependent potential

$$V^{\text{eff}}(r, E) = V_S(r) + V_V(r) + \frac{V_S(r)^2}{8\mu} - \frac{[E - V_V(r)]^2}{8\mu}, \quad (1.7)$$

where μ is the reduced mass and E the nonrelativistic energy. The author proves that, from $b\bar{b}$ to $u\bar{u}$ systems, V^{eff} does not appreciably differ from $V_S + V_V$ provided V_S contains a negative constant. He also gives some physical reasons which suggest the necessity of such a constant potential.

Bhaduri and Brack [9] have calculated the spectra of the one-body Dirac equation for a massless quark with different confining interactions. They show that it is possible to choose an effective mass and an effective potential

in a Schrödinger equation to reproduce quite well the relativistic spectra. Moreover, the Dirac magnetic moments may also be reasonably well reproduced by the Schrödinger formalism provided the nonrelativistic formula of the magnetic moment is modified for the excited states.

In the work of Gunion and Li [10], the spectra resulting from a relativistic treatment of a linear scalar confinement potential were calculated using one-body Klein-Gordon and Dirac wave equations. The authors show that, for a given choice of parameters and a given orbital angular momentum value, the Klein-Gordon and Dirac wave equations yield essentially identical spectra. Moreover, they show that these spectra do not differ very much from those of the nonrelativistic treatment for the first few low-lying states.

These studies shed some light on the connections existing between potential models with relativistic and nonrelativistic kinematics, but many points remain questionable. In the work of Lucha and Schöberl [6], only the semirelativistic approach is considered, and it is not clear that the effective Schrödinger Hamiltonian (1.2) is still relevant for nonlogarithmic potentials which could appreciably modify the effective masses and potential from one level to another. The duality relation found by Rosenstein [7] between Eqs. (1.4) and (1.5) concerns only one-body systems; moreover, the confining power-law potential, which yields the correct Regge trajectories for the relativistic equation of motion, is not quadratic but linear [11,12]. The work of Ono [8] is a two-body analysis, but the quarks are treated as spinless particles; the situation is exactly the opposite in the work of Bhaduri and Brack [9] and in the work of Gunion and Li [10].

In Ref. [13] the spectrum of the two-body Dirac equation was calculated with zero current masses and a linear scalar confining potential. It is shown that practically the same spectra can be obtained with a two-body Schrödinger equation using a wide range of potentials and constituent masses. In this paper, our purpose is to develop this work by comparing the spectra of nonrelativistic, semirelativistic, and relativistic potential models of quarkonium with a quark-antiquark interaction which is the sum of an attractive Coulomb potential and a confining power-law potential. Taking advantage of the scaling laws we point out results which are to a large extent independent of the parameters of the models. In Sec. II we present the three Hamiltonians with their specific scaling properties and we define a quantity suitable for measuring the difference between the spectra. Section III is devoted to an analytical comparison of the different models, which is possible when the interaction is reduced to a confining term. In Sec. IV, we carry out the comparisons for the complete Hamiltonians. Concluding remarks are presented in Sec. V.

II. MODELS AND SCALING LAWS

We consider three different models: nonrelativistic (N), semirelativistic (S) and relativistic (R). The relativistic model relies on the two-body Dirac formalism [12]. In the center-of-mass frame the corresponding Hamiltonians are given by

$$H_N = m_N(1) + m_N(2) + \frac{\mathbf{p}^2}{2\mu_N} + W_N(r) \quad (2.1)$$

$$\text{with } \mu_N = \frac{m_N(1)m_N(2)}{m_N(1) + m_N(2)},$$

$$H_S = \sqrt{\mathbf{p}^2 + m_S^2(1)} + \sqrt{\mathbf{p}^2 + m_S^2(2)} + W_S(r), \quad (2.2)$$

$$H_R = (\alpha_1 - \alpha_2) \cdot \mathbf{p} + \beta_1 m_R(1) + \beta_2 m_R(2) + W_R(r). \quad (2.3)$$

In these expressions, $\mathbf{p} = -i\nabla_{\mathbf{r}}$ is the conjugate momentum of the space variable $\mathbf{r} = \mathbf{r}_1 - \mathbf{r}_2$, and $r = |\mathbf{r}|$. The potential between the quark and the antiquark W_X (X denotes N , S , or R) contains a confining term $\lambda_X r^{a_X}$ supplemented by a Coulomb part $-\gamma_X/r$, which is the static interaction due to the one-gluon exchange ($\gamma = 4\alpha_s/3$, where α_s is the effective strong coupling constant which differs from one model to another). A constant potential Λ_X , which can be interpreted as a simple means to take into account unknown multigluon processes, is used to fix the ground state of the spectrum. Accordingly, for the Hamiltonians (2.1) and (2.2) the total potential is

$$W_X = -\frac{\gamma_X}{r} + \lambda_X r^{a_X} + \Lambda_X, \quad (2.4)$$

but for the relativistic model, the Lorentz character of the potential has to be specified. As the particles are only confined by scalar potentials, we can use a confining interaction which is proportional to the operator $\frac{1}{2}(\beta_1 + \beta_2)$ or $\beta_1\beta_2$. Although the expression $\beta_1\beta_2$ comes naturally from the reduction of the Bethe-Salpeter equation, we choose the other operator because it leads to simpler radial equations for the two-body Dirac equation. The Coulomb potential is due to one-gluon exchange, so it is treated as the time component of a four-vector potential. The constant potential is introduced in the same way since its function is to shift the entire spectrum. W_R is then given by

$$W_R = -\frac{\gamma_R}{r} + \frac{1}{2}(\beta_1 + \beta_2)\lambda_R r^{a_R} + \Lambda_R. \quad (2.5)$$

We study the solutions of these Hamiltonians by taking advantage of the scaling laws. We introduce a dimensionless space variable \mathbf{x} proportional to \mathbf{r} whose conjugate variable is $\mathbf{q} = -i\nabla_{\mathbf{x}}$ and a dimensionless mass κ_X . These quantities are defined by

$$\mathbf{x} = \begin{cases} (2\mu\lambda)^{1/(a+2)}\mathbf{r} & \text{for nonrelativistic model,} \\ \lambda^{1/(a+1)}\mathbf{r} & \text{for other models,} \end{cases} \quad (2.6)$$

$$\kappa_X(i) = m_X(i)\lambda_X^{-1/(a_X+1)}.$$

For the nonrelativistic model, the eigenenergies, which depend on the principal quantum number n and the total orbital angular momentum l , are given by the following formula

$$E_{n,l}^N = m_N(1) + m_N(2) + \Lambda_N + \left[\frac{\lambda_N^2}{(2\mu_N)^{a_N}} \right]^{1/(a_N+2)} \omega_{n,l}^N(a_N, \tau_N), \quad (2.7)$$

where $\omega_{n,l}^N$ is solution of the dimensionless equation

$$\left[\mathbf{q}^2 - \frac{\tau_N}{x} + x^{a_N} - \omega_{n,l}^N \right] \omega(\mathbf{x}) = 0, \quad (2.8)$$

and

$$\tau_N = \gamma_N \mathcal{R}_N^{(a_N+1)/(a_N+2)} \quad \text{with} \quad \mathcal{R}_N = \frac{2\kappa_N(1)\kappa_N(2)}{\kappa_N(1)+\kappa_N(2)}. \quad (2.9)$$

We remark that the mass dependence of the spectrum is very simple because the masses appear dynamically only through the reduced mass. Moreover, when $\gamma_N=0$, Eq. (2.8) is independent of the masses. This is a well-known peculiarity of the nonrelativistic model which is not present in the other models.

The eigenenergies of the semirelativistic Hamiltonian, which also depend only on n and l , are given by the formula

$$E_{n,l}^S = \Lambda_S + \lambda_S^{1/(a_S+1)} \omega_{n,l}^S(\kappa_S(1), \kappa_S(2), a_S, \gamma_S), \quad (2.10)$$

where $\omega_{n,l}^S$ is a solution of the dimensionless equation

$$\left[\sqrt{\mathbf{q}^2 + \kappa_S^2(1)} + \sqrt{\mathbf{q}^2 + \kappa_S^2(2)} - \frac{\gamma_S}{x} + x^{a_S} - \omega_{n,l}^S \right] \omega(\mathbf{x}) = 0. \quad (2.11)$$

The scaling laws for the relativistic model are the same as for the semirelativistic one. The corresponding eigenenergies are thus given by the formula

$$E_{\{t\}}^R = \Lambda_R + \lambda_R^{1/(a_R+1)} \omega_{\{t\}}^R(\kappa_R(1), \kappa_R(2), a_R, \gamma_R), \quad (2.12)$$

where $\omega_{\{t\}}^R$ is a solution of the spinorial dimensionless equation

$$\left[(\boldsymbol{\alpha}_1 - \boldsymbol{\alpha}_2) \cdot \mathbf{q} + \beta_1 \kappa_R(1) + \beta_2 \kappa_R(2) - \frac{\gamma_R}{x} + \frac{1}{2}(\beta_1 + \beta_2)x^{a_R} - \omega_{\{t\}}^R \right] \omega(\mathbf{x}) = 0 \quad (2.13)$$

and $\{t\}$ represents the set of quantum numbers which identify the states (total angular momentum J , parity P , and when they are well defined, total spin s and total orbital angular momentum l) [12]. As the Dirac equation (2.13) includes automatically spin effects, we define the centers of gravity $E_{n,l}^R$, which depend only on n and l , using the usual formula

$$E_{n,l}^R = \frac{\sum_J (2J+1) E_{\{t\}}^R}{\sum_J (2J+1)}, \quad (2.14)$$

where the sum \sum_J includes four levels (two levels only when $l=0$) characterized by the same principal quantum number n , and whose corresponding wave function is characterized either by a definite orbital angular momentum l [for states such that $P=(-1)^J$, $J=l$, and $s=0,1$] or by a dominant component with orbital angular momentum equal to l [for states such that $P=(-1)^{J+1}$,

$J=l\pm 1$, and $s=1$]. It can be checked numerically that the eigenenergies $E_{\{t\}}$ considered in sum (2.14) are nearly degenerate when γ_R is small (see Ref. [13] for the case $a_R=1$ and $\gamma_R=0$). The quantities $\omega_{n,l}^R$ are related to the eigenenergies $E_{n,l}^R$ by relation (2.12).

It is worth noting that the dimensionless levels $\omega_{n,l}^R$ and $\omega_{n,l}^S$ depend on four parameters while the quantities $\omega_{n,l}^N$ depend only on two parameters, and that, following formula (2.7), one of the two nonrelativistic masses can be chosen independently of the spectra, for instance to fix the magnetic moments of the baryons. In the nonrelativistic limit, the dimensionless levels are connected by the relation

$$\begin{aligned} \lim_{\kappa, \kappa' \rightarrow +\infty} [\omega_{n,l}^{R/S}(\kappa, \kappa', a, \gamma) - \kappa - \kappa'] \\ = \mathcal{R}^{-a/(a+2)} \omega_{n,l}^N(a, \gamma \mathcal{R}^{(a+1)/(a+2)}) \end{aligned} \quad (2.15)$$

with

$$\mathcal{R} = \frac{2\kappa\kappa'}{(\kappa + \kappa')}.$$

The difference between two spectra $\{E_{n,l}^X\}$ and $\{E_{n,l}^Y\}$ will be measured by calculating the average ‘‘gap’’

$$\Delta E^{X-Y} = \frac{1}{N_\Sigma} \sum_{n,l} |E_{n,l}^X - E_{n,l}^Y|, \quad (2.16)$$

where the sum includes N_Σ levels. This gap obviously depends on the states considered in the sum (2.16). In the following we shall only compare the lowest part of the different spectra. Accordingly, we shall consider all the states which are characterized by a number of quanta $N_Q = 2n + l$ below a given value N_Q^{\max} that we always take equal to 4, and thus $N_\Sigma = 9$.

III. COMPARISON WITH A CONFINING POTENTIAL ONLY

In this section we carry out analytical comparisons of the spectra of the nonrelativistic and semirelativistic Hamiltonians with the spectrum of the relativistic Hamiltonian taken as a reference spectrum. Our purpose is to point out the connections existing between the different spectra, knowing that the price to pay is possibly the use of approximate solutions or approximate Hamiltonians. The calculations are performed with the interaction reduced to a confining potential ($\gamma_X=0$) in cases where we can expect the largest differences between the models, that is to say, the $q\bar{q}$ system ($q=u$ or d) and the $q\bar{Q}$ system (Q is a very heavy-flavor quark). The mass of the q quark being generally taken very small in the models with relativistic kinematics, we assume that $m_R(q) = m_S(q) = 0$. It is then possible to express solutions of the different Hamiltonians in terms of the solutions $\eta_{n,l}(a)$ of the dimensionless equation

$$\left[\frac{d^2}{dy^2} - \frac{l(l+1)}{y^2} - y^a + \eta_{n,l}(a) \right] w(y) = 0, \quad (3.1)$$

where we have $\eta_{n,l}(2) = 4n + 2l + 3$, and $\eta_{n,0}(1)$ is the

$(n+1)$ th zero of the Airy function $\text{Ai}(x)$. An approximate formula for $\eta_{n,l}(a)$ with $a > 0$ exists [12], but we shall use the exact values of $\eta_{n,l}(a)$ obtained by numerical integration of (3.1).

A. $q\bar{q}$ system

For vanishing masses and Coulomb potential, the approximate solutions of Eq. (2.11) are [14]

$$\begin{aligned} \omega_{n,l}^S(\kappa_S(1)=0, \kappa_S(2)=0, a_S, \gamma_S=0) \\ = \left(\frac{a_S+1}{a_S} \pi(2n+l+\frac{3}{2}) \right)^{a_S/(a_S+1)}, \end{aligned} \quad (3.2)$$

and in Ref. [12] we find the approximate solutions of Eq. (2.13),

$$\begin{aligned} \omega_{n,l}^R(\kappa_R(1)=0, \kappa_R(2)=0, a_R, \gamma_R=0) \\ = 2^{a_R/(a_R+1)} \sqrt{\eta_{n,l}(2a_R)}. \end{aligned} \quad (3.3)$$

Obviously we have, exactly,

$$\omega_{n,l}^N(a_N, \tau_N=0) = \eta_{n,l}(a_N). \quad (3.4)$$

The exponents of the confining potentials are chosen in order to obtain the linear Regge trajectories in the different models. As $\lim_{l \rightarrow +\infty} \eta_{n,l}(a) \sim l^{2a/(a+2)}$ [12], we take $a_R = a_S = 1$ and $a_N = \frac{2}{3}$ (in agreement with Ref. [15]). Consequently, the spectra are given by the formulas

$$E_{n,l}^N = 2m_N(q) + \Lambda_N + \frac{\lambda_N^{3/4}}{m_N^{1/4}(q)} \eta_{n,l}(\frac{2}{3}), \quad (3.5)$$

$$E_{n,l}^S = \Lambda_S + \sqrt{\pi \lambda_S (4n+2l+3)}, \quad (3.6)$$

$$E_{n,l}^R = \Lambda_R + \sqrt{2\lambda_R (4n+2l+3)}. \quad (3.7)$$

The approximate spectrum of the semirelativistic model (3.6) coincides with the approximate spectrum of the relativistic model (3.7) if we take $\Lambda_S = \Lambda_R$ and $\lambda_S = (2/\pi)\lambda_R$. In this case $\Delta E^{R-S} = 0$. The situation is more complicated for the nonrelativistic spectrum. Setting $E_{0,0}^N = E_{0,0}^R$ and $E_{0,1}^N = E_{0,1}^R$, we obtain

$$\begin{aligned} 2m_N(q) + \Lambda_N = 0.241\sqrt{\lambda_R} + \Lambda_R, \\ \lambda_N^{3/4}/m_N^{1/4}(q) = 1.092\sqrt{\lambda_R}. \end{aligned} \quad (3.8)$$

With the conditions expressed above, we can write the eigenenergies in the form

$$E_{n,l}^X = \Lambda_R + \sqrt{\lambda_R} d_{n,l}^X, \quad (3.9)$$

where $d_{n,l}^X$ are dimensionless quantities given by

$$d_{n,l}^R = d_{n,l}^S = \sqrt{2} \eta_{n,l}^{1/2}(2), \quad (3.10)$$

$$d_{n,l}^N = 0.241 + 1.092 \eta_{n,l}(\frac{2}{3}). \quad (3.11)$$

We compare them in Fig. 1, where we can see that at least the highest level of each group with the same number of quanta nearly coincide for the three models. The gap between two spectra is then given by

$$\Delta E^{X-Y} = \sqrt{\lambda_R} \frac{1}{q} \sum_{N_Q=0}^4 |d_{n,l}^X - d_{n,l}^Y|. \quad (3.12)$$

As the slope of the Regge trajectories fixes the value of $\sqrt{\lambda_R}$ around 500 MeV, we find $\Delta E^{R-N} \simeq 45$ MeV. This result is to be compared with the lowest and highest levels of the relativistic spectra which are located, respectively, at 1225 and 2345 MeV when $\Lambda_R = 0$.

Two remarks must be made concerning these analytical results. First, the exact solutions, with the same excitation energy, for the relativistic and semirelativistic Hamiltonians with zero masses and linear confining potential are not degenerate. This is only the case for the approximate solutions (3.6) and (3.7). If we use the exact solutions of Eqs. (2.11) and (2.13), we find $\Delta E^{R-S} \simeq 63$ MeV instead of 0. This large discrepancy is due to the poor accuracy of formula (3.2). The use of exact solutions of Eq. (2.13) gives $\Delta E^{R-N} \simeq 37$ MeV, which is very close to the result found with approximate solutions (3.3). Second, the values chosen for the parameters a_N , a_S , and $m_S(q)$ are those which generate the linear Regge trajectories, that is to say, which minimize the gap between the levels of the different models in the region of large values of l . Consequently, they are certainly not the best values to minimize the gap defined in the previous section. Varying the values of a_N , a_S , and $m_S(q)$, we calculate new exact values of $d_{n,l}^X$, and we can then make ΔE^{R-N} as small as ~ 23 MeV for $a_N = 0.873$. In the same way, ΔE^{R-S} can be reduced to ~ 27 MeV with $m_S(q) \gtrsim 4\sqrt{\lambda_S}$. As we shall see in the next section, this last result is due to the fact that relativistic and semirelativistic spectra have different behaviors as a function of κ . The new dimensionless levels are presented in Fig. 2,

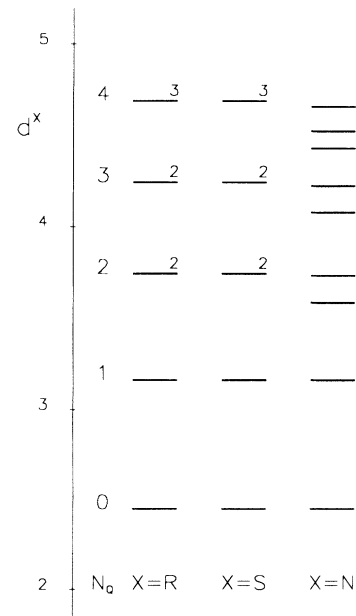


FIG. 1. Comparison between the dimensionless approximate $q\bar{q}$ spectra $\{d_{n,l}^R\}$, $\{d_{n,l}^S\}$, and $\{d_{n,l}^N\}$ including all the states with quantum numbers n and l such that $N_Q = 2n + l \leq 4$. A number above a level indicates its degeneracy with respect to n and l .

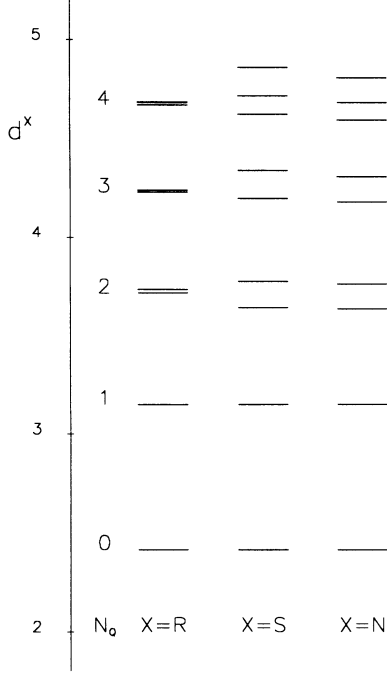


FIG. 2. Same as Fig. 1 but with exact values of $d_{n,l}^X$ for optimum values of parameters a_N , a_S , and $m_S(q)$ (see text).

where we can see that the centers of gravity of groups of levels with the same number of quanta coincide quite well for the three models.

The calculations are carried out by making the two first levels equal in the models. A better agreement between the spectra can be found by changing these two reference levels as is done in Ref. [13].

B. $q\bar{Q}$ system

Q being a very heavy-flavor quark, the Hamiltonians of the different models are written as follows

$$H_R = (\alpha_1 - \alpha_2) \cdot \mathbf{p} + \frac{1}{2}(\beta_1 + \beta_2)\lambda_R r^{a_R} + \beta_2 m_R(Q) + \Lambda_R, \quad (3.13)$$

$$H_S = \sqrt{\mathbf{p}^2} + m_S(Q) + \lambda_S r^{a_S} + \Lambda_S, \quad (3.14)$$

$$H_N = m_N(Q) + m_N(q) + \frac{\mathbf{p}^2}{2m_N(q)} + \lambda_N r^{a_N} + \Lambda_N. \quad (3.15)$$

The Hamiltonians (3.14) and (3.15) are approximate Hamiltonians obtained assuming that $m_S^2(Q) \gg \mathbf{p}^2$ and $\mu_N \simeq m_N(q)$. The approximate solutions of the Hamiltonian (3.13) are given in Ref. [12]. We have

$$E_{n,l}^R = m_R(Q) + \Lambda_R + \lambda_R^{1/(a_R+1)} [\eta_{n,l}(a_R)]^{(a_R+2)/(2a_R+2)}. \quad (3.16)$$

From formula (3.2), the approximate solutions of the Hamiltonian (3.14) are

$$E_{n,l}^S = m_S(Q) + \Lambda_S + \lambda_S^{1/(a_S+1)} \times \left[\frac{a_S+1}{2a_S} \pi(2n+l+\frac{3}{2}) \right]^{a_S/(a_S+1)}. \quad (3.17)$$

The solutions of the Hamiltonian (3.15) are given by

$$E_{n,l}^N = m_N(Q) + m_N(q) + \Lambda_N + \left[\frac{\lambda_N^2}{[2m_N(q)]^{a_N}} \right]^{1/(a_N+2)} \eta_{n,l}(a_N). \quad (3.18)$$

In the literature the quark masses are generally such that $m_N(Q) > m_S(Q) > m_R(Q)$ and $m_N(Q) \simeq m_R(Q) + m_N(q)$. We shall take $m_N(Q)$ and $m_S(Q)$ in terms of $m_R(Q)$ so that the ground states of the three models coincide. Expressing the links found between the parameters of the semi- and nonrelativistic models and the parameters of the relativistic one for the $q\bar{q}$ system, we obtain, with $a_R = a_S = 1$ and $a_N = \frac{2}{3}$,

$$E_{n,l}^X = m_R(Q) + \Lambda_R + \sqrt{\lambda_R} d_{n,l}^X, \quad (3.19)$$

with

$$d_{n,l}^R = \eta_{n,l}^{3/4}(1), \quad (3.20)$$

$$d_{n,l}^S = 0.159 + \eta_{n,l}^{1/2}(2), \quad (3.21)$$

$$d_{n,l}^N = 0.035 + 0.918 \eta_{n,l}(\frac{2}{3}). \quad (3.22)$$

The different definitions of the mass of the Q quark are then connected by the relations

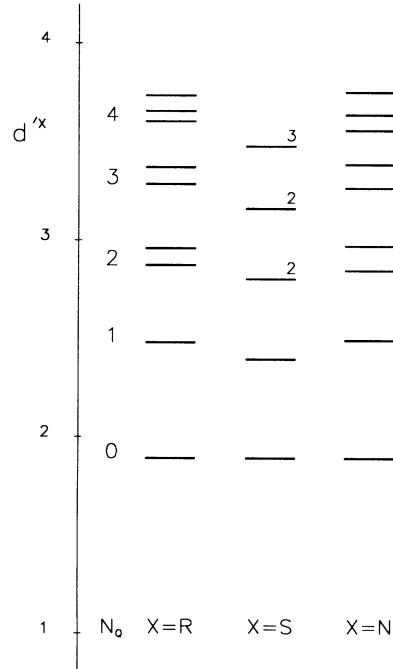


FIG. 3. Comparison between the dimensionless approximate $q\bar{Q}$ spectra $\{d_{n,l}^R\}$, $\{d_{n,l}^S\}$, and $\{d_{n,l}^N\}$ including all the states with quantum numbers n and l such that $N_Q = 2n + l \leq 4$. A number above a level indicates its degeneracy with respect to n and l .

$$m_S(Q) = m_R(Q) + 0.159\sqrt{\lambda_R}, \quad (3.23)$$

$$m_N(Q) = m_R(Q) + m_N(q) - 0.206\sqrt{\lambda_R}. \quad (3.24)$$

In Fig. 3 we compare the dimensionless quantities $d'_{n,l}$. We can see that the nonrelativistic spectrum is very similar to the relativistic one. The gap between the different spectra is given by formula (3.12) where we replace $d_{n,l}$ by $d'_{n,l}$. We find $\Delta E^{R-N} \simeq 9$ MeV, while the lowest and highest values of $E_{n,l}^R - m_R(Q) - \Lambda_R$ are, respectively, 945 and 1867 MeV. The agreement between the relativistic and the semirelativistic spectra is not so good; we find $\Delta E^{R-S} \simeq 67$ MeV.

IV. COMPARISON FOR COMPLETE HAMILTONIAN

As the one-gluon-exchange process has a large contribution to the meson masses, it is interesting to test to what extent the models can yield similar results when this interaction is turned on. In this section, we shall compare the low-lying levels of the three models with the complete Hamiltonian, but we shall restrict our calculations to systems composed of quarks with the same mass [$\kappa_X(1) = \kappa_X(2) = \kappa_X$]. The spectra are obtained by accurate numerical integration of the different equations of motion. For the relativistic model we only consider linear confinement in order to obtain good Regge trajectories. Consequently, the dimensionless levels $\omega_{n,l}^R$ depend only on κ_R and γ_R . As $\sqrt{\lambda_R}$ is around 0.5 GeV, we consider the levels $\omega_{n,l}^R$ with κ_R from 0 to 3 in order to include in our study the systems $q\bar{q}$ ($= u\bar{u}, d\bar{d}$), $s\bar{s}$, and $c\bar{c}$. The parameter γ_R is taken from 0 to 1.5, which covers reasonable values of the effective strong coupling constant. As the semirelativistic model is characterized by

dynamics similar to that of the relativistic model, we also consider only linear confinement and study the dimensionless levels $\omega_{n,l}^S$ with κ_S from 0 to 3 and γ_S from 0 to 1.5. For the nonrelativistic model we do not impose a fixed value for the exponent of the confinement, so the dimensionless levels $\omega_{n,l}^N$ depend on a_N and $\tau_N = \gamma_N \kappa_N^{(a_N+1)/(a_N+2)}$. We shall vary the value of a_N from 0 to 1.5 and the values of τ_N from 0 to 1.5, as $\kappa_N^{(a_N+1)/(a_N+2)} \simeq 1$ for most of the parameter values considered. A zero value for a_N means that the confining potential is logarithmic.

From formulas (2.7), (2.10), and (2.12) we can write, for each model considered

$$E_{n,l}^X = A^X + B^X \omega_{n,l}^X, \quad (4.1)$$

where A^X and B^X are quantities with the dimension of energy and where $\omega_{n,l}^X$ depend on dimensionless parameters. Whatever the values of $\omega_{n,l}^X$ may be, it is always possible to fix the values of two levels of the spectrum by a good choice of A^X and B^X . Consequently, instead of comparing the levels $E_{n,l}^X$ of two energy spectra, we shall compare the dimensionless quantities

$$R_{n,l}^X = \frac{E_{n,l}^X - E_{0,0}^X}{E_{0,1}^X - E_{0,0}^X} = \frac{\omega_{n,l}^X - \omega_{0,0}^X}{\omega_{0,1}^X - \omega_{0,0}^X}, \quad (4.2)$$

whose values are independent of A^X and B^X . Since we want to compare the lowest part of the different spectra, we choose the lowest levels $E_{0,0}$ and $E_{0,1}$ as the reference levels (for all the situations considered, the level with $n=0$ and $l=1$ is generally the first excited state). When two relative spectra $\{R_{n,l}^X\}$ and $\{R_{n,l}^Y\}$ are equal, the real

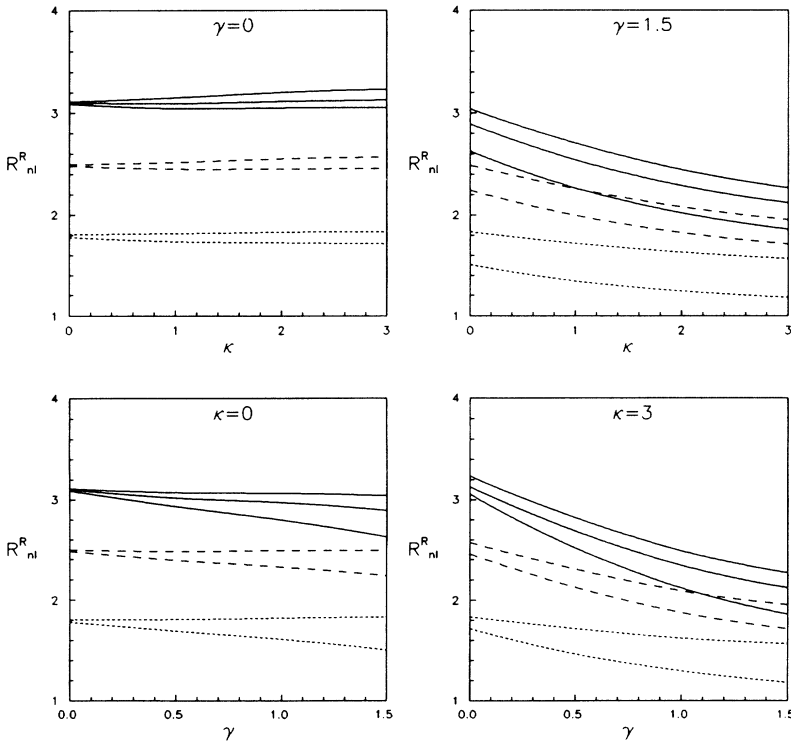


FIG. 4. Relative spectra $\{R_{n,l}^R\}$ of the relativistic model as a function of κ_R and γ_R . $2n+l=2$ for short-dashed curves, 3 for long-dashed curves, 4 for solid curves.

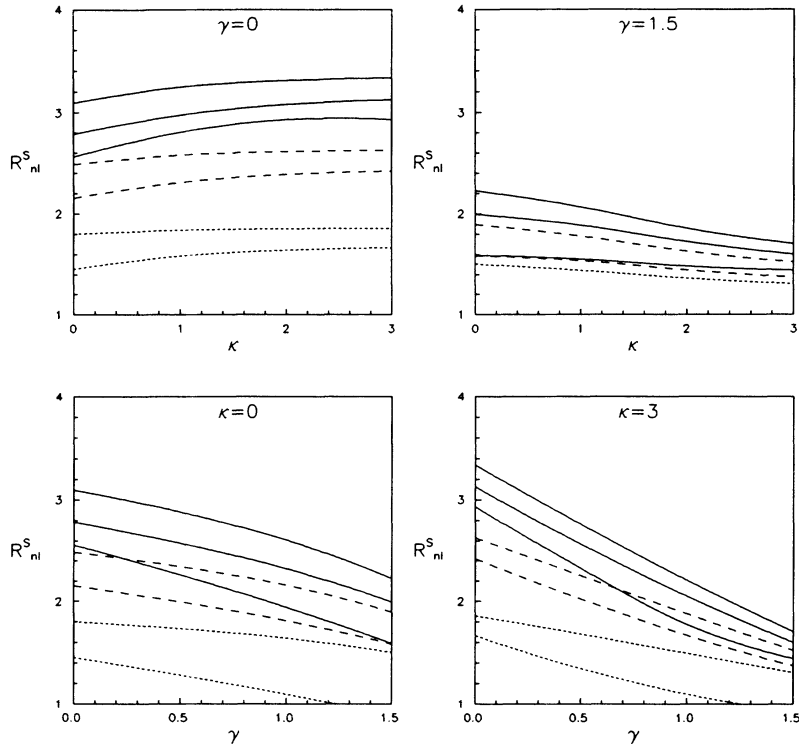


FIG. 5. Relative spectra $\{R_{n,l}^S\}$ of the semirelativistic model as a function of κ_S and γ_S . $2n+l=2$ for short-dashed curves, 3 for long-dashed curves, 4 for solid curves. Note that $R_{1,0}^S(0 \leq \kappa_S \leq 3, \gamma_S = 1.5) < 1$.

corresponding spectra $\{E_{n,l}^X\}$ and $\{E_{n,l}^Y\}$ can always be made equal too.

It is important to note that all the relevant characteristics of a spectrum are contained in the values of the relative levels $R_{n,l}$. The $R_{n,l}$ curves are thus universal curves and give the appearance of the spectra for a wide range of

physical parameters. In particular, the order of the levels is well determined, and the crossing points of levels could be expressed by relations between the physical parameters. Consequently, this formalism is a powerful tool to point out general characteristics of the models.

In Figs. 4–6 we present for the three models con-

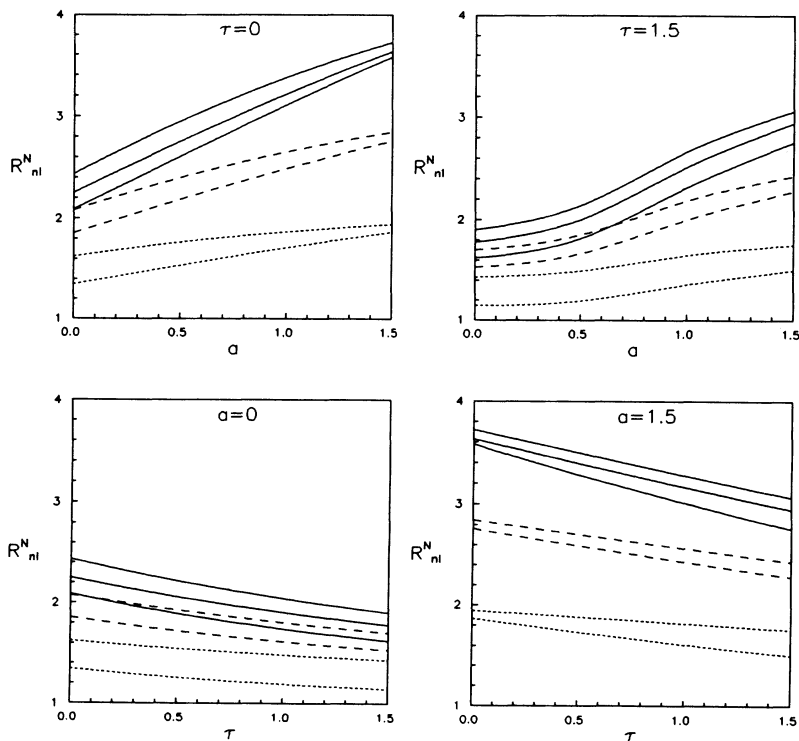


FIG. 6. Relative spectra $\{R_{n,l}^N\}$ of the non-relativistic model as a function of a_N and τ_N . $2n+l=2$ for short-dashed curves, 3 for long-dashed curves, 4 for solid curves.

sidered the values of $R_{n,l}$ for a number of excitation quanta $N_Q = 2n + l$ equal to 2, 3, and 4. In this work, the number of quanta, which is a rigorous notion only for an isotropic harmonic oscillator, is used as a convenient quantity to classify the levels. As we can see from the figures, the levels with the same excitation energy N_Q can be arranged in groups for some ranges of the parameters. Moreover, the spectra are always such that $R_{1,0} < R_{0,2}$ for $N_Q = 2$, $R_{1,1} < R_{0,3}$ for $N_Q = 3$, and $R_{2,0} < R_{1,2} < R_{0,4}$ for $N_Q = 4$; though some levels characterized by N_{Q+1} quanta can be located below levels characterized by N_Q quanta. Obviously, in the nonrelativistic model, the groups of levels are well distinguishable when τ_N is small and a_N quite large. We remark that for fixed values of κ and γ , the relative semirelativistic and relativistic spectra are clearly different. Crossings of levels appear with smaller values of γ for the semirelativistic spectra. Moreover, the separation between groups of levels increases with κ , whereas the situation is opposite for the relativistic spectra.

To carry out the comparisons, we choose a reference relative spectrum $\{R_{n,l}^X(p_X, q_X)\}$ which depends on two parameters p_X and q_X for a set of quantum numbers (n, l) such that $N_Q \leq N_Q^{\max} = 4$. Then we vary the two parameters p_Y and q_Y of another relative spectrum $\{R_{n,l}^Y(p_Y, q_Y)\}$ in order to minimize the quantity

$$\Delta R^{X-Y} = \frac{1}{9} \sum_{N_Q=0}^4 |R_{n,l}^X(p_X, q_X) - R_{n,l}^Y(p_Y, q_Y)|, \quad (4.3)$$

where the two spectra are such that $E_{0,0}^Y = E_{0,0}^X$ and $E_{0,1}^Y = E_{0,1}^X$. Obviously, the values of p_Y and q_Y that minimize ΔR^{X-Y} and the lowest value reachable for this quantity depend on the states we consider to carry out the comparison. Different results would be obtained by changing the two reference levels or by including in sum (4.3) more states than just those with the lowest number of quanta. We have from (4.2)

$$E_{n,l}^X - E_{n,l}^Y = (E_{0,1}^X - E_{0,0}^X)(R_{n,l}^X - R_{n,l}^Y). \quad (4.4)$$

The average gap between the two spectra $\{E_{n,l}^X\}$ and $\{E_{n,l}^Y\}$ is then given by

$$\Delta E^{X-Y} = (E_{0,1}^X - E_{0,0}^X) \Delta R^{X-Y}. \quad (4.5)$$

From experimental spectra, we can estimate that $E_{0,1} - E_{0,0}$ is around 400–600 MeV from $b\bar{b}$ to $q\bar{q}$ systems. In the following we always take the value 500 MeV for the theoretical differences $E_{0,1}^X - E_{0,0}^X$. Consequently, $\Delta R^{X-Y} \sim 10^{-2}$ yields an average gap between two spectra which is $\Delta E^{X-Y} \sim 5$ MeV.

All the calculations are carried out imposing the equality of the two levels $(n, l) = (0, 0)$ and $(0, 1)$. It is possible that another choice of the two reference levels could lower the gap between spectra [13]. Consequently, the values of ΔR^{X-Y} presented in the following must be considered as upper bounds of the minimal possible values.

A. Comparison between different nonrelativistic Hamiltonians

It has been stressed by Martin [16] that the quarkonium spectra in the nonrelativistic approach can be ob-

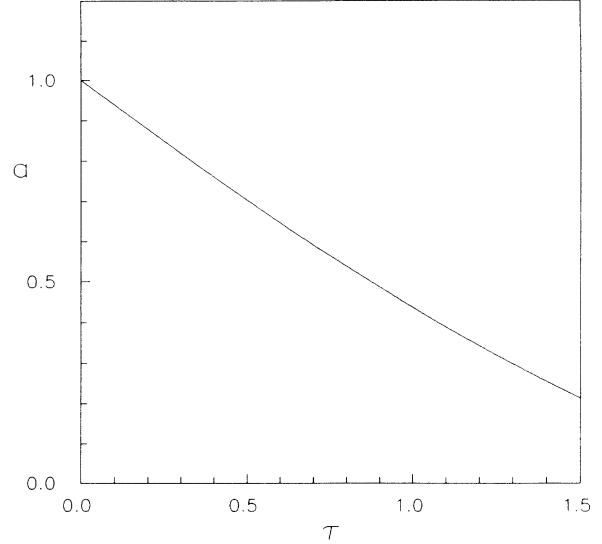


FIG. 7. Relation between the parameters a and τ , which minimize ΔR^{N-N} , calculated with $N_Q^{\max} = 4$ for the two relative spectra $\{R_{n,l}^N(a, \tau=0)\}$ and $\{R_{n,l}^N(a=1, \tau)\}$.

tained as well by the potential $V_1 = Ar^a + B$ with $a = 0.1$ as by the potential $V_2 = -\gamma/r + \lambda r$. We can check the similarity of the two corresponding spectra by comparing the relative spectra $\{R_{n,l}^N(a, \tau=0)\}$ and $\{R_{n,l}^N(a=1, \tau = \gamma R^{2/3})\}$. For a given value of τ for V_2 , we calculated the value of a for V_1 which minimizes the gap ΔE^{N-N} between the spectra of each Hamiltonian. We found that for τ varying from 0 to 1.5, ΔR^{N-N} is always below 2.3×10^{-2} . So the average gap is less than 12 MeV. Figure 7 shows the ideal values of a which minimize the gap as a function of τ . We present in Fig. 8 the relative spectra $\{R_{n,l}^N(a=1, \tau=0.7)\}$ and $\{R_{n,l}^N(a=0.592, \tau=0)\}$ for which ΔR^{N-N} is 1.4×10^{-2} .

In fact, the equivalence between spectra yielded by po-

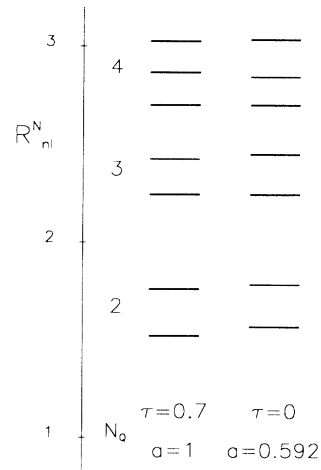


FIG. 8. Comparison between the two relative spectra $\{R_{n,l}^N(a=1, \tau=0.7)\}$ and $\{R_{n,l}^N(a=0.592, \tau=0)\}$ for which $\Delta R^{N-N} = 1.4 \times 10^{-2}$. All levels such that $2 \leq N_Q = 2n + l \leq 4$ are shown.

tentials V_1 and V_2 is very good for a wide range of the exponent of V_1 , provided a peculiar relation exists between the parameters of the two interactions.

B. Comparison between nonrelativistic and other spectra

For given values of κ_R and γ_R of the relativistic Hamiltonian, we calculated values of a_N and τ_N of the nonrelativistic Hamiltonian which minimize the gap ΔE^{R-N} . Actually, for some values of the relativistic parameters, very similar values of the gap can be obtained with different couples (a_N, τ_N) . In Table I are shown only the nonrelativistic parameters which yield the absolute minima of the gap. We can see that for reasonable values of $\gamma_R \sim 0.5-1$, the agreement between the two spectra is good, especially for large values of the quark mass. We compare in Tables II and III the relative spectra $R_{n,l}^R$ and $R_{n,l}^N$, which give respectively the worst and best values obtained for the average gap. We can remark that some nonrelativistic levels are in better agreement with their relativistic counterparts than others. From Table I it is apparent that no universal values of a_N and τ_N exist which minimize the gap. These parameters are very sensitive to the values of κ_R and γ_R . However, it is worth noting that for $0.5 \leq \gamma_R \leq 1$, the values found for a_N are located between $\sim \frac{2}{3}$ and ~ 1 , which are the values commonly used for confining potentials in nonrelativistic models.

The nonrelativistic spectra were also compared with the semirelativistic ones. The results, which are given in Table IV, show that the agreement between the spectra is reasonable, but not as good as in the case of the comparison with the relativistic spectra. Some large values of ΔR^{S-N} present in Table IV are due to the fact that we did not consider values of τ_N greater than 1.5.

TABLE I. Values of a_N and τ_N of the nonrelativistic Hamiltonian which minimize the gap ΔE^{R-N} , calculated with $N_Q^{\max}=4$, as a function of the parameters κ_R and γ_R of the relativistic Hamiltonian. The quantity ΔR^{R-N} is also shown. An asterisk indicates that a lower value of ΔR^{R-N} could be found with $\tau_N > 1.5$.

$\kappa_R \backslash \gamma_R$	0	1	2	3
1.5	$a_N=1.113$ $\tau_N=0.864$ $\Delta R^{R-N}=0.028$	0.818 1.029 0.028	0.766 1.500* 0.025	0.572 1.385 0.023
1.0	0.687 0.000 0.017	0.785 0.642 0.009	0.778 1.084 0.007	0.809 1.500* 0.008
0.5	1.000 0.393 0.038	0.728 0.184 0.021	0.689 0.296 0.012	0.833 0.748 0.008
0.0	1.354 0.857 0.064	1.177 0.557 0.044	1.087 0.355 0.031	1.076 0.307 0.024

TABLE II. Relative spectra $\{R_{n,l}^R(\kappa_R=0, \gamma_R=0)\}$ and $\{R_{n,l}^N(a_N=1.354, \tau_N=0.857)\}$ for which $\Delta R^{R-N}=6.4 \times 10^{-2}$, and estimation of the difference δ in MeV between the absolute corresponding levels $E_{n,l}^R$ and $E_{n,l}^N$ using $E_{0,1}-E_{0,0}=500$ MeV. ΔR^{R-N} is calculated with $N_Q^{\max}=4$.

N_Q	n	l	$R_{n,l}^R$	$R_{n,l}^N$	δ (MeV)
2	1	0	1.779	1.596	91.4
	0	2	1.807	1.807	0.0
3	1	1	2.482	2.393	44.5
	0	3	2.497	2.540	21.5
4	2	0	3.089	2.951	69.0
	1	2	3.104	3.104	0.0
	0	4	3.111	3.230	59.3

C. Comparison between semirelativistic and relativistic spectra

Solutions of Hamiltonians (2.2) and (2.3) have the same Regge trajectories $E_{n,l}^2 \sim l^{2a/(a+1)}$ for light quarks interacting only via a confining potential λr^a and have the same nonrelativistic limit apart from spin effects; but their spectra can be very different, especially when a Lorentz-vector interaction is turned on (see Figs. 4 and 5). In Table V we calculated the values of κ_S and γ_S which minimize the gap ΔE^{R-S} for given values of κ_R and γ_R . The two spectra can be made similar but, as expected from the analysis of Figs. 4 and 5, with values of semirelativistic parameters which are not the same as their relativistic counterparts. Lowest values of ΔE^{R-S} are generally found for $\kappa_S > \kappa_R$ and $\gamma_S < \gamma_R$, that is to say, when the semirelativistic model is close to the nonrelativistic one. Thus, the physical meaning of the parameters in these two models might certainly be very different: for instance, current quark mass values for relativistic models such as the Dirac equation, and well-fitted constituent quark mass values for semirelativistic Hamiltonians.

V. CONCLUSIONS

The success of the description of mesons and baryons by relativistic as well as by nonrelativistic potential quark models is a very intriguing situation [6–10]. Developing

TABLE III. Relative spectra $\{R_{n,l}^R(\kappa_R=2, \gamma_R=1)\}$ and $\{R_{n,l}^N(a_N=0.778, \tau_N=1.084)\}$ for which $\Delta R^{R-N}=0.7 \times 10^{-2}$, and estimation of the difference δ in MeV between the absolute corresponding levels $E_{n,l}^R$ and $E_{n,l}^N$ using $E_{0,1}-E_{0,0}=500$ MeV. ΔR^{R-N} is calculated with $N_Q^{\max}=4$.

N_Q	n	l	$R_{n,l}^R$	$R_{n,l}^N$	δ (MeV)
2	1	0	1.363	1.363	0.0
	0	2	1.674	1.650	12.1
3	1	1	1.981	1.981	0.0
	0	3	2.195	2.179	8.2
4	2	0	2.277	2.285	4.1
	1	2	2.493	2.477	8.3
	0	4	2.637	2.639	0.9

TABLE IV. Values of a_N and τ_N of the nonrelativistic Hamiltonian which minimize the gap ΔE^{S-N} , calculated with $N_Q^{\max}=4$, as a function of the parameters κ_S and γ_S of the semirelativistic Hamiltonian. The quantity ΔR^{S-N} is also shown. An asterisk indicates that a lower value of ΔR^{S-N} could be found with $\tau_N > 1.5$.

$\gamma_S \backslash \kappa_S$	0	1	2	3
1.5	$a_N=0.495$	0.351	0.000	0.000
	$\tau_N=1.500^*$	1.500*	1.500*	1.500*
	$\Delta R^{S-N}=0.081$	0.056	0.075	0.013
1.0	0.798	0.766	0.658	0.540
	1.500*	1.500*	1.500*	1.500*
	0.080	0.053	0.035	0.029
0.5	0.705	0.753	0.379	0.766
	0.698	0.657	0.120	0.858
	0.066	0.043	0.032	0.020
0.0	0.839	0.735	0.846	0.897
	0.557	0.000	0.000	0.000
	0.049	0.029	0.017	0.018

a previous analysis of this feature [13], we have compared the spectra of nonrelativistic, semirelativistic, and relativistic quark-antiquark Hamiltonians with a reasonable QCD-inspired interaction.

In a first step, we have considered the case of a purely confining potential with the zero-mass approximation for the light quark (q) in relativistic dynamics. By means of analytical results, we showed the following.

(i) The $q\bar{q}$ spectra for the three different dynamical models considered can be made very similar provided appropriate connections exist between the physical parameters.

(ii) The similarities between spectra are widely preserved for systems containing a light quark and a heavy-flavor antiquark, although the parameters used are fixed from the $q\bar{q}$ system.

As is apparent from relations (2.7) and (3.8), the nonrelativistic light-quark mass $m_N(q)$ can be fixed independently of the energy spectrum of the $q\bar{q}$ system, thanks to the presence of an adjustable constant potential.

In a second step, we have turned on a Coulomb attractive interaction. Removing the physical parameters by the appropriate scaling laws, we pointed out results which are applicable to a wide variety of quarkonia. Provided particular relations exist between the physical parameters of the models to be compared, we found the following.

(i) The nonrelativistic spectra obtained either by a

TABLE V. Values of κ_S and γ_S of the semirelativistic Hamiltonian which minimize the gap ΔE^{R-S} , calculated with $N_Q^{\max}=4$, as a function of the parameters κ_R and γ_R of the semirelativistic Hamiltonian. The quantity ΔR^{R-S} is also shown. An asterisk indicates that a lower value of ΔR^{R-S} could be found with $\kappa_S > 3$.

$\gamma_R \backslash \kappa_R$	0	1	2	3
1.5	$\kappa_S=1.396$	1.063	1.393	2.748
	$\gamma_S=0.222$	0.636	0.919	0.932
	$\Delta R^{R-S}=0.018$	0.022	0.027	0.018
1.0	1.754	3.000*	2.947	2.960
	0.109	0.380	0.558	0.700
	0.033	0.021	0.018	0.019
0.5	2.059	3.000*	3.000*	3.000*
	0.002	0.226	0.315	0.390
	0.059	0.039	0.030	0.026
0.0	2.463	2.258	2.718	3.000*
	0.000	0.000	0.000	0.000
	0.081	0.061	0.049	0.043

power-law potential plus a constant or by a linear confining potential plus a Coulomb attractive interaction can be nearly the same.

(ii) The relativistic spectra for linear confining plus Coulomb attractive potentials and the nonrelativistic spectra for power-law confining plus attractive Coulomb potentials compare quite well for relevant values of the dimensionless parameters peculiar to each model.

(iii) The mass dependence of the semirelativistic spectra is very different from that of the relativistic spectra, and consequently, it does not compare very well with relativistic and nonrelativistic spectra.

From this work, we cannot conclude that one of the models considered is preferable, but it is generally recognized that models with relativistic dynamics are more rigorous from the theoretical point of view. Our hope is that the good equivalence found between relativistic and nonrelativistic spectra for two-quark systems persists for multi-quark systems. In that case, the reliability of the nonrelativistic quark model, which can be more easily extended to multibody dynamics than relativistic models, would be reinforced.

ACKNOWLEDGMENTS

We would like to thank Professor R. Ceuleneer for helpful discussions. One of us (C.S.) would like to thank the F.N.R.S. for financial support.

[1] Yu. A. Simonov, Nucl. Phys. **B324**, 67 (1989); Phys. Lett. **B 226**, 151 (1989).
[2] M. Fabre de la Ripelle and Yu. A. Simonov, Ann. Phys. (N.Y.) **212**, 235 (1991).
[3] D. B. Lichtenberg, Int. J. Mod. Phys. A **2**, 1669 (1987).
[4] D. D. Brayshaw, Phys. Rev. D **36**, 1465 (1987).
[5] S. Godfrey and N. Isgur, Phys. Rev. D **32**, 189 (1985); S.

Capstick and N. Isgur, *ibid.* **34**, 2809 (1986).
[6] W. Lucha and F. F. Schöberl, Phys. Rev. Lett. **64**, 2733 (1990).
[7] B. Rosenstein, Phys. Rev. D **33**, 813 (1986).
[8] S. Ono, Phys. Rev. D **26**, 2510 (1982).
[9] R. K. Bhaduri and M. Brack, Phys. Rev. D **25**, 1443 (1982).

- [10] J. F. Gunion and L. F. Li, *Phys. Rev. D* **12**, 3583 (1975).
- [11] C. Goebel, D. LaCourse, and M. G. Olsson, *Phys. Rev. D* **41**, 2917 (1990).
- [12] C. Semay, R. Ceuleneer, and B. Silvestre-Brac, Université de Mons-Hainaut report (unpublished).
- [13] R. Ceuleneer, P. Legros, and C. Semay, in *On the Connection Between Relativistic and Nonrelativistic Descriptions of Quarkonium*, Proceedings of the European Workshop on Hadronic Physics with Electrons beyond 10 GeV, Dourdan, France, 1990, edited by B. Frois and J.-F. Mathiot [*Nucl. Phys.* **A532**, 395c (1991)].
- [14] P. Cea, P. Colangelo, G. Nardulli, G. Preparata, and G. Paiano, *Phys. Rev. D* **26**, 1157 (1982).
- [15] M. Fabre de la Ripelle, *Phys. Lett. B* **205**, 97 (1988).
- [16] A. Martin, *Phys. Lett.* **100B**, 511 (1981).